Supplemental Data

Characterization and Coding

of Behaviorally Significant Odor Mixtures

Jeffrey A. Riffell,[1,*] Hong Lei,[1] Thomas A. Christensen,[1,2] and John G. Hildebrand

Supplemental Experimental Procedures

Floral odor collection and analysis and behavioral experiments

Odor collection

Floral scent was collected from *D. wrightii* plants using dynamic headspace sorption. The floral scent previously was characterized by GCMS [1,2]. In the present study, we wished to make our own absolute determinations. To accomplish this, living flowers in field populations were enclosed in transparent vinyl oven bags (Reynolds) cinched at 500-mL volumes with plastic ties. Portable diaphragm vacuum pumps (KNF Neuberger, Trenton, NJ, USA) were used to pull fragrant headspace air through sorbent cartridge traps at a flow rate of 250 mL air/min. Odor traps were constructed by packing 100 mg of Super Q adsorbent (mesh size 80–100) into borosilicate glass tubes (7 mm) plugged with i.d.#4 silanized glass wool. Scent collections began at anthesis (near sunset for all plants) and continued overnight for up to 12 h. Twenty replicates of floral volatiles were collected from twenty individuals of *D. wrightii*.

Odor analysis

Trapped volatiles were eluted from sorbent cartridges using 400 µL of HPLC grade hexane. Each sample was stored in 2 mL borosilicate glass vials with Teflon-lined caps

at -80 °C until analysis. 1 µL of the volatile sample was injected into and analyzed using a GC–time-of-flight mass spectrometry (TOF-MS) system consisting of an HP 6890 (Agilent Technologies, Palo Alto, CA, USA) gas chromatograph and a Waters TOF-MS (Waters-Micromass, Millford, MA, USA). A DB5 (30 m, 0.25 mm, 0.25 µm) (J&W Scientific, Folsom, CA, USA) column was used. Helium was used as a carrier gas at constant flow of 1 ml/m. The initial oven temperature was 50° C for 5 min followed by a heating rate of 6° C per min until 230° C was reached and held isothermally for further 6 min. Eluated peaks were tentatively identified using TOF-MS with 70 eV electron impact ionization and comparison with the NIST mass spectral library (ca. 120,000 spectra) and verification by chromatography with authentic standards (when available) or known components of essential oils. Peak areas for each compound were integrated using MicroMass MassLynx software and are presented in terms of relative abundance as percent of total fragrance emitted. Odorant peak areas for each species were quantified using the internal standards and expressed in units of nanograms per flower per hour. The *D. wrightii* floral scent contains up to 80 individual odorants. In this study, we examined only those peaks that elicited significant neural responses (z-scores ≥ 2.0) or for which the tentative identity could be determination from the mass spectra, thus limiting the total number of odorants to ca. 60.

Behavioral experiments

Two different series of experiments were performed to determine the behavioral efficacy of the mixture and single-odorant stimuli. The first series of experiments was performed in a wind tunnel where each odor stimulus was tested singly. This allowed a forced-

choice test of the behavioral efficacy of the single odorants and mixtures. The second series of experiments was performed in a flight arena where moths were exposed to two different treatments in a two-choice test. In contrast to the wind-tunnel experiments, the two-choice experiments allowed direct comparison between the moth's preferences for flowers emitting the live *D. wrightii* odor versus flowers emitting the *D. wrightii* mixture mimic. All behavioral experiments were conducted at the beginning of scotophase with naïve, 3 day old adult male moths.

Behavioral experiments using a wind tunnel. The wind tunnel simulates important aspects of the physical (air speed and turbulence) and odor environments normally encountered by *M. sexta* moths. For our experiments, the physicochemical environment of the wind tunnel was scaled to simulate naturally turbulent conditions in the field [3] and the odor emissions of *D. wrightii* flowers (Tables S1 and S2.). A nine-component mixture of odorants identified as AL-active was prepared using purified synthetic standards and tested for behavioral activity on male moths in a wind tunnel: The mixture was prepared by adding each component at a concentration that approximated that found in the *D. wrightii* floral headspace collections, with a total blend concentration of 6.25 ng/ml air ± 1.29 SEM as quantified through GC-FID. 25 µL aliquots of the mixture and mixture constituents (at equal concentration to that found in the mixture) were pipetted onto a conical paper flower similar to those of [4]. In addition, mixture dilutions of 0.3, 0.1, 0.01, 0.003, and 0.001 were tested. Equal volume of mineral oil was used as a negative control. Serving as a positive control, a freshly cut *D. wrightii* flower was placed in sealed 3 L glass jar outside of the wind tunnel. Charcoal filtered air was

pumped into the jars at 0.02 L/min, and allowed to exit through 2 m long Teflon tubing (2 mm I.D.) connected to a paper flower in the wind tunnel. Flower odor emitted at this flow rate, trapped and quantified by GC (FID detection), produced emissions similar to those from natural flowers [2]. Last, to determine whether other odorants in the *D. wrightii* headspace might be behaviorally active irrespective of their elicited neural responses in the AL, a synthetic mixture was created with odorants characterized from the *D. wrightii* headspace and are also known to elicit responses in *M. sexta* ORCs and AL PNs (Table S2) [5,6].

The efficacy with which the synthetic mixture and individual odorants elicited oriented flight and foraging behavior of *M. sexta* males to the upwind odor source was tested in a Plexiglas wind tunnel (L × W × H = 4.0 × 1.5 × 1.5 m). Air was forced into the upwind end of the tunnel through a carbon filter and exhausted at the downwind end through a duct vented into a laboratory fume hood. As measured by a 3D sonic anemometer sampling at 32 Hz, the wind speed was 25 cm/s and turbulent wind intensities of 0.004 N/m^2 along the principle (*u*) axis. For each stimulus, a paper flower containing a 25 µL stimulus aliquot was placed in the upwind region of the wind tunnel. Males were tested individually by placing a moth, confined in a wire cage covered at both ends by plastic petri plates, on a platform located at the downwind end of the tunnel. The moth was permitted a 1.5-min acclimation period, after which the petri plates were removed and the moth was allowed to fly. Only moths that initiated wing-fanning and flight were used in the analyses. A total of 680 moths were used in wind tunnel experiments. 50 moths per mixture concentration and mineral oil control, and 20 moths per mixture constituent excepting the single odorants *bol* and *bea* in which 50

moths were tested. In addition, 20 moths were tested with the random mixture and *D. wrightii* scent, and 50 moths were tested with a two-component mixture of *bea*+*bol*.

Two types of behavioral data were acquired from the wind tunnel experiments: (1) video acquisition and subsequent motion analysis of moth flight behavior for each treatment group (detailed below), and (2) scoring of moth behaviors (flower contact and feeding). Video images of the moth flight tracks were captured by an overhead CCD camera with a macrolense (4m by 4m area) and recorded on analog video. The video was digitized and analyzed by a video-acquisition and motion analysis system (Peak3D, v7.2, Peak Motus Systems Inc., Los Angeles, CA, USA) with the subsequent flight tracks analyzed for ground speed, angular direction relative to odor source, rate change in direction, and odor-source visitation (defined by hovering and/or proboscis extension).

Flight arena two-choice experiments. To establish the behavioral efficacy of the nine-component mixture relative to the odor from a live *D. wrightii* flowers, we performed two-choice tests with laboratory-reared male moths that had eclosed 3 d prior to testing. At no time prior to experimentation were moths exposed to plant odor. Each moth was used only once, and released alone into the flight arena used for the two-choice tests. Twenty-six moths were used for each two-choice treatment. To test the foraging behaviors of *M. sexta* moths to paper flowers emitting the *D. wrightii*- and *D. wrightii* mixture mimic odors, moths were exposed to one of three treatments: (*i*) *D. wrightii* floral odor vs. nine-component *D. wrightii* mimic; (*ii*) *D. wrightii* floral odor vs. paper flower (no odor) control; or (*iii*) nine-component *D. wrightii* mimic vs. paper flower (no

odor) control. Flowers were randomly positioned in the flight arena and spaced 1 m apart. Paper flowers were white paper cones with an opening 8 cm in diameter and a length of 18 cm and served as a neutral visual display. As in the wind tunnel experiments, a freshly cut *D. wrightii* flower was each placed in sealed 3 L glass jar outside of the flight arena. Charcoal filtered air was pumped into the jars at 0.02 L/min and out through Teflon tubing (2 mm I.D., 2 m long) connected to a paper flower in the flight arena. For the nine-component *D. wrightii* mimic, a 25 µL aliquot of the mixture was loaded onto the paper flower. An equal volume of mineral oil was used as a negative control. Experiment (*i*) tested whether the moths have a preference between the two floral odors. Experiments (*ii*) and (*iii*) tested whether moths had the same level of preference for the single odor-laden flower.

Experiments were conducted by releasing single moths into a flight arena (1.8×1.8×1.8 m) containing the two treatments. Behaviors noted were the flower at which the first proboscis extension and active feeding took place and the number of proboscis extensions into the floral corollas. Each trial was 10 minutes in duration or lasted until the moth stopped flying for more than 3 min. The moth was then removed from the cage, and after an interval of at least 5 min, another moth was released. Flowers were replaced after every trial. From the number of proboscis extensions ("probes") into the flower corollas an Attraction Index was calculated by $(\#Probes_{FlowerA} - \#Probes_{FlowerB})/(Total\#Probes)$.

Behavioral data analysis and statistics. The percentage of responsive moths to each odor stimulus was plotted (e.g., Fig. 2A,B) and the effects of mixture concentration was

analyzed using a one-way ANOVA. Studies have shown that it is permissible to use an ANOVA on dichotomous data under certain conditions which are met by the experiments conducted in this study: at least 40 *df* of the error term and equal cell frequencies [7,8]. The α level was set to 0.05. Because the number of tested moths were unequal between certain odor stimuli (e.g., mixture and the single odorants) we used *G*-tests for all further between-group comparisons where the significance threshold was corrected using the Dunn-Sidak correction ($\alpha' = 1 - (1 - \alpha)^{1/k}$ where *k* is the number of comparisons in which each dataset is used) in order to reduce the type I errors [8,9].

Electrophysiology

Experimental preparation

Adult male moths (*Manduca sexta*; Lepidoptera: Sphingidae) were reared in the laboratory on an artificial diet [10] under a long-day (17/7 hr light/dark cycle) photoperiod. Animals were prepared for experiments 2–3 d after emergence, as described previously [11,12]. In preparation for recording, the moth was secured inside a plastic tube with dental wax, leaving the head and antennae exposed. The head was opened to expose the brain, and the tube was fixed to a recording platform attached to the vibration–isolation table. The preparation was oriented so that both ALs faced upward, and the tracheae and sheath overlying one AL were carefully removed with a pair of fine forceps. The brain was superfused slowly with physiological saline solution (in mM: 150 NaCl, 3 CaCl2, 3 KCl, 10 N-tris[hydroxymethyl] methyl-2

aminoethanesulfonic acid buffer, and 25 sucrose, pH 6.9) for the duration of the experiment.

Olfactory stimulation

Olfactory stimuli were delivered to the preparation by two different methods. The first method is use of a gas chromatogram. A 1 μL sample of collected headspace volatiles was injected (splitless, 30 s) into a Shimadzu model 14A GC (Columbia, MD, USA) equipped with a flame ionization detector (FID) and a DB-1 column. Effluent was split 1:1 between the FID of the GC and the moth antenna using a universal glass “Y” connector (J&W Scientific). Deactivated, fused-silica capillary tubing of the same internal diameter as the separation column carried the effluent to each detector. Effluent to the antenna passed through a heated transfer line (Syntech, Hilversum, Netherlands) set at 250° C and entered a 16-mm diameter glass tube via a small hole in the wall of the glass tube. Effluent to the antenna was mixed with a stream of charcoal-filtered, humidified air that flowed through the glass delivery tube at a rate of 800 ml/min (Fig. 1A).

The second method has been reported previously [13] where pulses of air from a constant air stream were diverted through a glass syringe containing a piece of filter paper on which was deposited a floral odor compound. The odor stimulus was pulsed by means of a solenoid-activated valve controlled by an electronic stimulator (W-P Instruments, Sarasota, FL). In each experiment, the outlet of the stimulus syringe was positioned 2 cm from and orthogonal to the center of the antennal flagellum ipsilateral to the AL. Stimulus duration was 200 ms, and five pulses were separated by a 5 s interval.

Three classes of olfactory stimuli were used: (1) aromatics: benzyl alcohol (*bol*), methyl salicylate (*mal*), and benzaldehyde (*bea*); (2) monoterpenoids: (±) linalool (*lin*), nerol (*ner*), *β*-myrcene (*myr*), and geraniol (*ger*); and (3) sesquiterpeniods: *α*-farnesene (*far*) and *trans-β*-caryophyllene (*car*). In addition, a mixture of all the odorants at the same concentrations, and 50 µL of floral extract were used. The control solvent for floral synthetic volatiles and synthetic blend was mineral oil (control), and for the floral extract was hexane (hex). A total of 16 adult moths were used in multi-unit recording experiments (detailed below). The first 8 moths (n = 121 units) were exclusively used in GCMR experiments and stimulated with the effluent from the GC. The next 8 moths (n = 113 units) were stimulated both with the effluent from the GC, as well as synthetic odor stimuli.

AL Ensemble recording system

The spatial distribution design of this MR (a 4 × 4 array) suits the dimensions of the AL in *M. sexta* (Fig. S10). These probes have four shanks spaced 125 µm apart, each with four recording sites 50 µm apart. The MR was positioned under visual control using a stereo microscope. The four shanks were oriented in a line parallel to the antennal nerve, with the first shank inserted into the macroglomerular complex and the remaining shanks into the isomorphic glomeruli. The MR was advanced slowly through the AL using a micromanipulator (Leica Microsystems, Bannockburn, IL) until the uppermost recording sites were just below the surface of the AL. In this manner, the four shanks of the MR recorded from four regions of glomerular neuropil across the AL. Ensemble activity was recorded simultaneously from the 16 channels of the MRA using two Lynx-8

amplifiers (Neuralynx, Tucson, AZ). Spike data were extracted from the recorded signals and digitized at 25 kHz per channel using Discovery acquisition software (Data Wave Technologies, Longmont, CO) and a 2821-G 16SE analog-to-digital board (Data Translation, Marlboro, MA) on a personal computer platform (Data Wave Technologies). Filter settings (typically 0.6–3 kHz) and system gains (typically 5,000 –20,000) were software adjustable on each channel. Spikes were sorted using a clustering algorithm based on the method of principal components (PCs) (Off-line Sorter; Plexon, Dallas, TX). Only those clusters that were separated after statistical verification in three dimensional (PC1–PC3) space (multivariate ANOVA; $P < 0.05$) were used for additional analysis (10–20 units were isolated per ensemble; $n = 16$ ensembles in as many animals) (Fig. S10B). Spikes arising from the same unit were visible on adjacent recording sites, thus providing geometric information about the spatial origin of the signals. Each spike in each cluster was time-stamped, and these data were used to create raster plots and to calculate peristimulus time histograms (PSTHs), interspike interval histograms, cross-correlograms, and rate histograms. All analyses were performed with Neuroexplorer (Nex Technologies, Winston-Salem, NC) using a bin width of 5 ms, unless noted otherwise.

Data analysis

Odor-evoked activity. Sorted units were arranged according to which of the four AL shanks (I–IV) defined by the MR yielded each recording (Fig. S10B). For each unit sorted, PSTHs were generated for all responses to each odor stimulus and the control (solvent only) stimulus. The response window was defined as the 400 ms period

beginning at the onset of the 200 msec stimulus pulse. A unit was considered to be responsive if its control-subtracted PSTH was above (excitatory) or below (inhibitory) the 95% confidence limits derived from a cumulative sum (CUMSUM) test. Inspection of the entire 113 unit data set revealed that a 400 ms window was sufficient to capture all of the stimulus-evoked responses recorded. We quantified the control corrected response for every unit by calculating a response index (RI) similar to that used in [9]. RI values reflect the deviation from the mean response of all units across all odors in one ensemble, as:

$$RI = (R_{odor} - R_m)/SD, \quad \text{(S1)}$$

where R_{odor} is the number of spikes evoked by the test odor minus the number evoked by the control stimulus, R_m is the mean response, and SD is the standard deviation across the data matrix. The RI values for the nonresponsive units fell between -2.0 and +2.0, based on the CUMSUM test. Given that 50% (on average) of recorded units in each ensemble were unresponsive, R_m approximated the background activity level, and thus negative values of the RI indicated response suppression. The RI values for all units were color-coded and arranged as an activity matrix with each row representing the ensemble response to a different odor stimulus. The RI had a range from -3.0 SDs (strongly inhibited units; cool colors) to +3.0 SDs (strongly excited units; warm colors).

Conditional response probability. To assess the validity of the arbitrary grouping of chemical classes and to examine the response preference of each unit for certain

olfactory stimuli, we calculated the conditional probability of response to all members of the stimulus set [12,14]. First, we grouped together all units that responded to a particular stimulus (P_A; reference stimulus), then calculated the probability that this subset of units also responded to the remaining members of the stimulus set *i*...*n* (comparison stimuli), where:

$$P_i/P_A = N_{i/A}/N_A \quad , \qquad \text{(S2)}$$

where $N_{i/A}$ was the number of *i*-responsive units within the pool of A-responsive units, and N_A was the total number of A-responsive units. If two odorants activated the same pool of units, the conditional probability for the two odorants would be 1.0. To summarize results for the entire data set, the conditional probability scores for all olfactory stimuli were color-coded and displayed in a response–probability matrix. The response matrices between the GC-effluent and synthetic standards were correlated to verify dynamic response similarity in the ensemble.

Mixture interactions and profile similarity. To determine how unit responses to individual odorants may differ from mixture-evoked responses, we used a categorization similar to [15]. In that study, mixture responses were compared to responses of the most-effective odorant. For each odorant and mixture tested, we thus categorized each unit in one of three different categories: mixture responses may be equal to ("hypoadditivity"), lower ("suppression"), or higher ("synergy") than the individual odorant producing the highest response. In addition, the number of units which were non-responsive was also

determined. Based on the average unit responses from each of the individual odorants (SEM = ca. 8%), a minimum difference of 8% was used for categorization.

Ensemble and unit synchrony. To calculate the temporal relationship between each pair of units, we used a crosscorrelation analysis using the following formula:

$$\mathrm{SI\%} = \frac{[SE]_{\mathrm{RAW}} - [SE]_{\mathrm{SHUFFLED}}}{N_1(T) + N_2(T)} \times 100 \qquad \text{(S3)}$$

where $[SE]_{\mathrm{RAW}}$ is the number of coincident events in the 5 ms crosscorrelogram peak centered around t = 0, and $[SE]_{\mathrm{SHUFFLED}}$ is the number of coincident events after trial shuffling (shift predictor method) to correct for coincidences attributable to chance and an increased firing rate [16]. The corrected correlograms were calculated by averaging over four trial shifts and subtracting the result from the raw correlogram. T is the total response time over which spikes were counted (400 ms), and N_1 and N_2 are the total number of spikes recorded from units 1 and 2 during time T. The synchrony index (SI%) therefore reflects the percentage of synchronous spikes relative to the total number of spikes recorded from the two neurons. All calculations were implemented in Matlab 7.02 (The Mathworks, Natick, MA) or Neuroexplorer (Nex Technologies). To visualize the odor-dependent coactivity pattern within an ensemble, we arranged individual units in a circular array used to describe ensemble patterns [12,17]. Each pair of units was connected with a line that depicted the magnitude of the correlation (SI%): values from 10–15%, dotted line; values 15-20%, dashed line; 20-30%, dashed line; and values >30%, solid line. In addition, each unit was color-coded to reflect its response

magnitude, and these values were used to make a direct comparison between the spatial and temporal activity patterns evoked by different odorants.

Ensemble response similarity to odor pairs. To compare between ensemble representations of different odor stimuli, two different analyses were used. The first analysis was the correlation coefficient between ensemble responses to two different stimuli (detailed below). The second analysis examined the relationship between odor-evoked responses of different stimuli in multivariate space through the normalized Euclidean distances between odors (Dissimilarity Index) (detailed below). These analyses were performed for the ensemble response indices (RIs) and the synchrony coefficients between cell pairs in the ensemble. Thus, these two different measures, correlation coefficient and Dissimilarity Index, together provide the means in which to examine the relationships between odor-evoked responses.

Correlation coefficient between odor pairs. To measure the ensemble-wide similarity between coactivity patterns evoked by different olfactory stimuli, we transformed the coactivity patterns composed of positive SI% values for all unit pairs in each ensemble into one-dimensional vectors (one for each odorant). The vectors were compared through a correlation coefficient:

$$r = \frac{SI_{i,j}}{\left(SI_{i,i}SI_{j,j}\right)^{-1/2}} \quad , \quad \text{(S4)}$$

where $SI_{i,i}$ and $SI_{j,j}$ are the two coactivity pattern vectors and $SI_{i,j}$ the mean subtracted cross-product of the two vectors resulting in a 0 - 1.0 correlation coefficient. A similar analysis was performed by transforming the RI values of individual units in each ensemble into one-dimensional vectors (one for each odorant: $RI_{i,i}$ and $RI_{j,j}$), and subsequently compared through correlative analysis. In this manner, the spatial distribution of activated units *versus* temporal activity patterns could be compared based on their resulting correlation coefficients between stimuli. Population data were calculated only within, not between, ensembles.

Dissimilarity Indices between odor pairs. The neural representation of each odorant and mixture was also examined in multidimensional space, where each dimension is represented by a certain unit of the ensemble. Since the number of units in the ensemble (10 – 20 units; 45-190 unit pairs) and the number of odor stimuli (n = 15) make it difficult to plot the vectors in 10-190 dimensional space, a principal-components analysis was used that identifies orthogonal axes (factors) of maximum variance in the data, and thus projects the data into a lower-dimensionality space formed of a subset of the highest-variance components. The first two factors (accounting for 82.1% of the total variance in RI values, ±2.98% SEM; 69.9% of the total variance in SI ±5.99% SEM) were then plotted. Finally, to evaluate the relationships between the representations of the mixture and the representation of its components, we calculated how close they were to each other in the putative olfactory space by calculating their Euclidian distance, d, in the n-dimensional space

$$d_{ij} = \sqrt{\sum_{k=1}^{p}(X_{ik} - X_{jk})^2} \qquad \text{(S5)}$$

where *i* and *j* indicating odors, *p* the number of dimensions, i.e. units, and X_{ik} the response in unit (or unit pair) *k* to odor *i*. Normalization of the Euclidean distances provided Dissimilarity Indices (0 – 1.0) between all odor pairs. The Dissimilarity Indices were thus calculated between all mixture pairs and mixtures and single odorants. This analysis was conducted separately for ensemble RI values, and ensemble SI values between unit pairs. Population data were calculated only within, not between, ensembles.

The Procrustes Analysis and determination of synchronous cell pairs used to encode mixture stimulus. To identify the relevant cell pairs which may encode the mixture stimulus, we used a Procrustes Analysis (PA) [18,19]. The PA has been widely used in the field of sensory biology and in comparison to other multivariate analyses (e.g., PCA) does not provide dimensional reduction of large data sets through orthogonal linear transformation. Instead, the PA is a procedure that minimizes the sum-of-squared differences between two configurations (i.e., data matrices) in a multivariate Euclidean space. The PA attempts to match one vector to another vector through matrix translation, scaling, and rotation. Here, the vector representing the SI% for all cell pairs in response to stimulation from the 10^0 odor mixture represented the reference matrix (*X*) and the other SI% vectors from the other mixture stimuli represented the rotation matrix (*Y*). Computationally, the Procrustean fit can be achieved by centering and scaling the two matrices by:

$$X_{scl} = (I - P)X / \sqrt{trace\left[(I - P)X'(I - P)\right]} \quad , \quad \text{(S6)}$$

where I is an (n×n) identity matrix and P is a (n×n) matrix with all elements = 1/n [15,16]. This step is repeated for the matrix Y to yield the rotated and scaled Y_{scl}. Output from this analysis provided two important variables, the first being a measure of the goodness of fit error (residual sum of squares error) which allowed an ANOVA to be conducted to determine the statistical similarity of SI% response matrices between stimuli. The second output variable of this analysis was a measure of goodness-of-fit for the SI% values for each cell pair between stimuli (larger values = better fit). Thus, this analysis provided identification of the cell pairs which responded similarly to the two stimuli.

We examined the importance of the cell pairs which responded similarly to the mixtures by removing the cell pairs and observing how similar the ensemble synchrony patterns were as a result. This was carried out separately for each ensemble (N = 8). We used three different algorithms to remove cell pairs from the ensembles. For random removal [20] we removed increasing proportions of all cell pairs chosen at random and replaced them with 0 (i.e., no synchronous activity). This process was repeated 100 times for each ensemble. Random removal represents a 'null model' with which to contrast two types of systematic removal, in which cell pairs were removed according to their similarity in evoked synchronous activity. We systematically removed cell pairs from those that were not contributing to the ensemble SI% response pattern (non-essential); and conversely, from the cell pairs which were contributing to the SI%

pattern (as determined by the PA). The first approach examines the importance of cell pairs which have dissimilar evoked synchronous activity to the different stimuli. The second approach explores the 'tolerance' of ensembles to loss of highly connected nodes [20].

Histological identification of recording probe locations

To examine the precise location of the recording probes, the brain was excised and immersed in 1–2% glutaraldehyde in 0.1 M phosphate buffer to increase tissue contrast and facilitate locating probe tracks. Brains (n = 8) were fixed for 6 - 12 h, then dehydrated with a graded ethanol series, cleared in methyl salicylate, and finally imaged as whole mounts with a laser-scanning confocal microscope (Zeiss 510 Meta equipped with a 457 nm argon laser). Optical sections were 1 µm, and this method reliably revealed the tracks of the four MR shanks in the AL without the need for tissue staining (Fig. S10). To examine consistency of the MR probe position in the AL, confocal image stacks were reconstructed and analyzed using Amira v.4.1.2 (Indeed-Visual Concepts, Houston TX). Glomerular structures in the AL were labeled as previously described [21] with the boundaries between adjacent glomeruli determined by the "4viewer" mode which allows assessment of the glomerular structure in all possible 2D planes of each respective image stack (Fig. S10C,D). The glomeruli adjacent to, and impaled by, each shank were color-coded: blue for shank 2, yellow shank 3, and green for shank 4. Shank 1 was placed in the MGC region of the AL. In addition, the Cumulus macroglomerulus (C-MGC) and Toroid macroglomerulus 1 and 2 (T-MGC) were reconstructed. The relative positions of the labeled isomorphic glomeruli with respect to

the MGC glomeruli allowed comparison between preparations. 3-dimensional reconstructions of the impaled and neighboring glomeruli provided determination of the consistency between preparations on the location of the recording sites. While identification of individual glomeruli is an important prerequisite for assigning functional significance to a given glomerulus, this is beyond the scope of this study.

Supplemental Data – Results

Synthetic versus headspace odorants determined by GCMR

To verify the identity of the group of odorants (*bea, bol, mal, myr, lin, ner, ger, car*, and *far*) determined by GCMR which elicited robust responses in neurons of the moth's AL, and their effectiveness in evoking unit responses, synthetic standards of the nine compounds were tested and compared to the natural GC-eluted odorants in 8 of the 16 ensembles. Units that responded to two of the headspace odorants, *myr* and *bol*, also responded vigorously to their synthetic homologues (Fig. S3A). Headspace odorants generally eluted over a prolonged time period (~ 2-12 s), and thus the unit responses to natural stimuli had longer durations than responses to the synthetic stimuli that were delivered in 200 ms odor pulses. Nonetheless, the peak firing rates evoked by natural and synthetic homologues of the same odorant were comparable. In addition, we compared the response profile of an entire ensemble to the suite of the same nine odorants in their headspace and synthetic forms. The results show that the two odorant formulations produced similar population-response profiles (Fig. S3B; Spearman's rank correlation test: $r_s = 0.87$, $P < 0.0001$).

To determine whether the equivalent effectiveness of headspace and synthetic stimuli was consistent across ensembles and animals, and to examine whether ensemble-response patterns could be classified by chemical class, conditional response probabilities were calculated for all units in every ensemble (a total of 113 units in eight moths). A group of units that showed an excitatory response to *lin* also showed similar responses to *ner* (also an oxygenated monoterpenoid), but these units were less responsive to aromatics (Fig. S3C). Moreover, sesquiterpenes and monoterpenes also shared similar potency in activating the same group of units, with the odorants far and car (sesquiterpenes) and *ger* and *ner* (monoterpenes) eliciting similar unit responses. The same trend was found with the synthetic odorants, where units responsive to *lin* also responded to *ner* (Fig. S3C, right). Therefore, both synthetic and headspace odorants produced similar patterns of conditional response probability (Spearman's rank correlation test: $r_s = 0.95$, $P < 0.0001$), suggesting a similar effectiveness of these two types of stimuli in producing the ensemble responses.

Pairwise stimulus correlations from spatiotemporal neural responses

To determine the relative contribution between spatial and temporal population activity for mixture and intensity coding, we first investigated the spatial distribution of activated units in response to mixtures or single odorants. At the single-unit level, at least in some units, mixture-evoked responses could be predicted by the unit's response to the dominant constituent of the blend (e.g. *bol*), as shown in Fig. S6A. However, predictability was dependent on mixture concentration: a 100-1000 fold dilution markedly diminished the response similarity between *bol* and the mixture. To further

quantify the similarity between mixture- and single odorant-evoked ensemble activity patterns, pair-wise correlations were made between all mixtures, and mixtures versus single odorants for eight preparations (see Fig. 4B for single preparation example). Results demonstrated that the most concentrated mixtures (10^0 to 10^{-2}) were significantly more correlated to one another than to the individual odorants (Fig. S6B; Mann-Whitney *U*-test: $P < 0.01$). The most dilute mixture (10^{-3}), but one that still evokes behavior, did not produce ensemble response patterns that were significantly different from those seen to the individual odorants (Fig. S6B; Mann-Whitney *U*-test: $P > 0.05$). These results suggest that the spatial distribution pattern of ensemble responses alone does not fully explain the consistent behavior across this concentration range.

We next examined how the temporal activity of the ensemble, through synchrony, may represent the mixtures with changing concentration relative to the single odorants. From the ensemble synchrony patterns, pair-wise correlations were made between all mixtures, and mixtures versus single odorants for eight preparations (see Fig. 4A,E,F for single preparation example). From the population data, results demonstrate that mixtures were significantly more correlated than the single odorants in all preparations (Fig. S6C; Mann-Whitney *U*-test: $P < 0.05$, $n = 8$ moths), again suggesting a qualitative difference between mixture (regardless of concentration) and the single odorant-evoked synchrony patterns.

Supplementary Data – Reference List

1. Raguso R.A., Henzel C., Buchman S.L., and Nabhan G.P. (2003). Trumpet flowers of the Sonoran Desert: floral biology of Peniocereus Cacti and Sacred Datura. I. J. Plant Sci. *164*: 877-892.

2. Riffell J.A., Alarcon R., Abrell L., Davidowitz G., Bronstein J.L., and Hildebrand J.G. (2008). Behavioral consequences of innate preferences and olfactory learning in hawkmoth-flower interactions. PNAS *105*: 3404-3409.

3. Riffell J.A., Abrell L., and Hildebrand J.G. (2008). Physical processes and real-time chemical measurement of the insect olfactory environment. J. Chem. Ecol. *34*: 837-853.

4. Raguso R.A. and Willis M.A. (2005). Synergy between visual and olfactory cues in nectar feeding by wild hawkmoths, *Manduca sexta*. Animal Behaviour *69*: 407-418.

5. Reisenman C.E., Christensen T.A., and Hildebrand J.G. (2005). Chemosensory selectivity of output neurons innervating an identified, sexually isomorphic olfactory glomerulus. J. Neurosci. *25*: 8017-8026.

6. Shields V.D.C. and Hildebrand J.G. (2001). Responses of a population of antennal olfactory receptor cells in the female moth *Manduca sexta* to plant-associated volatile organic compounds. J. Comp. Physiol. [A] *186*: 1135-1151.

7. Lunney G.H. (1970). Using analysis of variance with a dichotomous dependent variable: An empirical study. J. Educ. Meas. *7*: 263–269.

8. Guerrieri F., Schubert M., Sandoz J.C., Giurfa M. (2005). Perceptual and neural olfactory similarity in honeybees. PLoS Biol. *3*: e60.

9. Jones D. (1984). Use, misuse, and role of multiple-comparison procedures in ecological and agricultural entomology. Envir. Entomol. *13*: 635-649.

10. Bell R.A. and Joachim F.G. (1976). Techniques for rearing laboratory colonies of tobacco hornworms and pink ballworms. Ann. Entomol. Soc. *69*: 365-373.

11. Christensen T.A., Pawlowski V.M., Lei H., and Hildebrand J.G. (2000). Multi-unit recordings reveal context-dependent modulation of synchrony in odor-specific neural ensembles. Nat. Neurosci. *3*: 927-931.

12. Lei H., Christensen T.A., and Hildebrand J.G. (2004). Spatial and temporal organization of ensemble representations for different odor classes in the moth antennal lobe. J. Neurosci. *24*: 11108-11119.

13. Christensen T.A., Waldrop B.R., Harrow I.D., and Hildebrand J.G. (1993). Local interneurons and information processing in the olfactory glomeruli of the moth *Manduca sexta*. J. Comp. Physiol. [A] *173*: 385-399.

14. Fletcher M.L. and Wilson D.A. (2003). Olfactory bulb Mitral-Tufted cell plasticity: odorant-specific tuning reflects previous odorant exposure. J. Neurosci. *23*: 6946-6955.

15. Duchamp-Viret P., Duchamp A., and Chaput M.A. (2003). Single olfactory sensory neurons simultaneously integrate the components of an odour mixture. Euro. J. Neurosci. *18*: 2690-2696.

16. Aertsen A.M., Gerstein G.L., Habib M.K., and Palm G. (1989). Dynamics of neuronal firing correlation: modulation of “effective connectivity”. J. Neurophysiol. *61*: 900-917.

17. Wilson M.A. and McNaughton B.L. (1994). Reactivation of hippocampal ensemble memories during sleep. Science *265*: 676-679.

18. Peres-Neto P. and Jackson D. (2001). How well do multivariate data sets match? The advantages of a Procrustean superimposition approach over the Mantel test. Oecologia *129*: 169-178.

19. Rohlf F.J. and Slice D. (1990). Extensions of the Procrustes Method for the Optimal Superimposition of Landmarks. Syst. Zool. *39*: 40-59.

20. Albert R., Jeong H., and Barabasi A.L. (2000). Error and attack tolerance of complex networks. Nature *406*: 378-382.

21. Galizia C.G., McIlwrath S.L., and Menzel R. (1999). A digital three-dimensional atlas of the honeybee antennal lobe based on optical sections acquired by confocal microscopy. Cell Tissue Res. *295*: 383-394.

Supplemental Data – Tables

Table S1. Volatile headspace constituents from *D. wrightii* identified by GCMS. Compounds are listed in order of GC retention time. Determined by comparison to spectra in the National Institute of Standards and Technology (NIST) ’98 spectral library and by comparison of spectra and retention times with standard samples. Confirmed by accurate mass measurement (observed mass within 5 mDa of calculated mass). Compounds in bold are those verified with synthetic standards.

Peak/Odorant no. Fig. 1	Ret. t. (min)	Putative compound	Emission rate (ng/min)	Structure class
1	3.62	**2-hexanone**	0.54	AP
3	3.75	3-propyl cyclopentene	1.76	AP
4	4.01	3-ethyl cyclopentene	0.05	AP
5	4.02	3-[2-propenyl]-1-cyclopentene	0.05	AP
6	4.31	3-oxatricyclononane	0.02	AP
7	4.56	cyclobutanespiro-2-bicyclobutane	0.04	AP
8	4.69	2-ethoxyethyl benzene	0.05	AR
9	4.81	2-8-decadiyne	0.04	AP
10	4.87	1-methylethyl benzene	0.03	AR
11	4.97	Unk.	0.04	AR
12	4.87	Unk.	0.04	AR
13	4.93	Unk. AR: *m/z:* [45], 77, 84, 105, 120	0.01	AR
14	5.13	1-ethyl, 4-methyl benzene	0.04	AR
15	5.22	3-propyl cyclopentene	0.03	AP
16	5.5	3-ethyl cyclopentene	0.03	AP
17	5.58	3-[2-propenyl]-1-cyclopentene	0.04	AP
18	6.43	3-oxatricyclononane	0.28	AP
19	6.54	cyclobutanespiro-2-bicyclobutane	0.20	AP
20	6.96	2-ethoxyethyl benzene	0.05	AR
21	7.27	*m/z*: [59], 77, 93, 106	0.04	MO
22	7.51	*m/z:* [45], 77, 84, 105, 120	0.08	AR
23	7.58	*m/z:* 45, 77, 84, 91, [105], 120	0.29	AR
24	8.00	*m/z*: 45, [67], 77, 91, 105	0.10	MO
25	8.18	*m/z*: 45, 53, [67], 77, 91, 105	0.20	MO
26	8.38	*m/z*: 53, 68, 77, [93], 108, 136	0.17	MO
27	8.68	**sabinene**	0.25	MO

28	8.89	*m/z*: 77, [93], 108, 136	0.25	MO
30	9.33	*m/z:* 59, 77, [93], 105	0.20	MO
31	9.62	***cis*-3-hexenyl acetate**	0.05	AP
33	9.87	**α-phellandrene**	0.13	MO
34	10.40	**limonene**	0.14	MO
	10.59	**1,8 cineole**	0.17	MO
35	11.01	*β*-ocimene	45.03	MO
36	11.24	**allo-ocimene**	0.04	MO
37	11.30	myrcenol	0.04	MO
38	11.4	p-Mentha-1(7),8(10)-dien-9-ol	0.08	MO
39	11.52	**methyl benzoate**	0.48	AR
40	12.14	4,6,6-trimethyl-Bicyclohept-3-ene-2-acetaldehyde	0.08	MO
41	12.25	*m/z*: 53, 67, 79, [91], 119, 134, 156	0.08	MO
42	12.47	*m/z*: 65, 77, 91, [119], 134, 152	0.03	MO
43	12.55	4,7,7-trimethyl-Bicyclohept-4-en-3-ol	0.06	MO
44	12.73	1,3,8-p-menthatriene	0.07	MO
45	13.68	phenylmethyl acetate	0.11	AR
46	13.81	*m/z*: 51, 65, 77, 91, 105, [119], 134	0.03	MO
47	15.01	**geranial**	0.74	MO
48	15.34	**neral**	0.12	MO
49	16.52	**geranyl acetate**	0.02	SE
50	18.44	*m/z*: 53,79,93,107,[119],134,150, 175	0.03	SE
51	19.91	**benzyl benzoate**	0.04	AR
50	21.7	*m/z*: 51,67,77,93,105, [119], 136, 207	0.10	SE
51	21.9	Unk.	0.10	AL
52	8.52	**benzaldehyde**	0.23	AR
53	10.27	**benzyl alcohol**	5.99	AR

54	13.5	**methyl salicyclate**	1.68	AR
55	9.7	***β*-myrcene**	0.59	MO
56	12.75	**linalool**	0.24	MO
57	14.1	**nerol**	1.24	MO
58	14.6	**geraniol**	26.71	MO
59	17	***E*-caryophyllene**	0.04	SE
60	17.8	***α*-farnesene**	0.83	SE

Table S2. Liquid-phase constituent concentrations in mixtures. Constituents of the random mixture was chosen using a random numbers generator from those odorants identified from the *D. wrightii* floral headspace by GCMS and present in a odorant library of more than 200 odorants. The random mixture contains odorants of the same chemical class as those in the synthetic *D. wrightii* mimic (e.g., terpenoids and aromatics), and was tested at an equal concentration (based on vapor pressure and verified by GC-FID).

Mixture	Odorant	Concentration (µg)	Purity (%)
Synthetic *D. wrightii*			
	Benzaldehyde (*Bea*)	0.50	≥99.5 [Fluka]
	Benzyl alcohol (*Bol*)	122.24	≥99.8 [Sigma]
	Methyl salicylate (*Mal*)	0.67	≥99.5 [Fluka]
	β-Myrcene (*Myr*)	0.04	≥95.0 [Fluka]
	Linalool (*Lin*)	0.90	≥97.0 [Aldrich]
	Nerol (*Ner*)	17.80	≥97.0 [Aldrich]
	Geraniol (*Ger*)	724.40	≥99.0 [Fluka]
	E-Caryophyllene (*Car*)	8.10	≥98.5 [Fluka]
	Farnesene (Far)	4.20	≥90.0 [Fluka]
Random mixture			
	Z-3-Hexen-1-ol	0.02	≥98.0 [Fluka]
	Methyl benzoate	1.0	≥98.5 [Fluka]
	α-phellandrene	0.01	≥95.0 [Fluka]

Sabinene	0.08	≥97.0 [Fluka]
Allo-ocimene	0.08	80.0 [Aldrich]
β-ocimene	30.0	≥90.0 [Fluka]
Geranyl acetone	0.33	≥98.0 [Fluka]
2-hexanone	0.01	98.0 [Sigma]
Farnesol	0.33	≥95.0 [Aldrich]

Table S3. one-way ANOVA with post-hoc Fisher's test assessing the effects of mixtures, single odorants, and mineral oil control (Ctl.) on moth feeding responses. Only those single odorants that elicited a feeding response by the tested moths (*bea* and *bol*), and the two-component mixture of *bea* and *bol*, were used in the ANOVA.n = 50 moths per treatment.

Factor (d.f.)	Summed square	*F*-value	*P*-value
Olfactory stimulus (9)	13.16	8.78	<0.0001
Residual (490)	81.58		

Fisher's test (feeding effect):

	Behaviorally effective mixtures									
Stimulus:	**1.0**	**0.3**	**0.1**	**0.01**	**0.003**	**0.001**	***bea+bol***	***bea***	***bol***	**Ctl.**
1.0	-									
0.3	>0.99	-								
0.1	>0.99	0.62	-							
0.01	0.62	0.62	>0.99	-						
0.003	>0.99	>0.99	0.62	0.62	-					
0.001	0.46	0.46	0.22	0.22	0.46	-				
bea+bol	<0.001	<0.001	<0.0001	<0.0001	<0.001	<0.01	-			
bea	<0.0001	<0.0001	<0.0001	<0.0001	<0.0001	<0.01	0.62	-		
bol	<0.001	<0.001	<0.0001	<0.0001	<0.001	<0.01	0.80	0.80	-	
Ctl.	<0.0001	<0.0001	<0.0001	<0.0001	<0.0001	<0.0001	0.22	0.46	0.32	-

Values are the *P*-value from the Fisher's test.

Supplemental Data – Figures

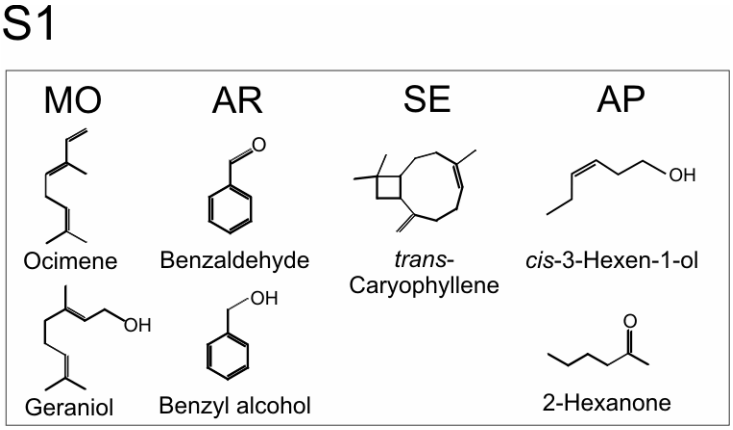

Fig. S1. The *D. wrightii* flower produces a chemically diverse fragrant scent containing: monoterpenoids (MO) such as *trans*-*β*-ocimene and geraniol; aromatics (AR) like benzyl alcohol and benzaldehyde; sesquiterpenoids (SE) including *E*-caryophyllene and *α*-farnesene; aliphatics (AP) such as *cis*-3-hexen-1-ol and 2-hexanone.

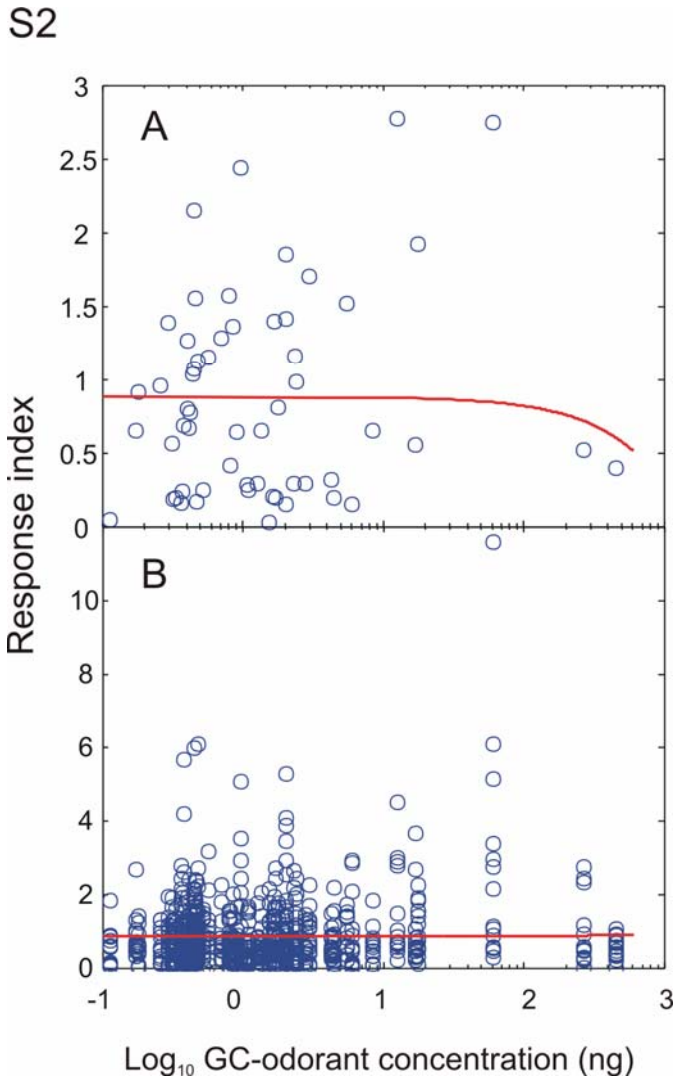

Fig. S2. Unit and ensemble responses to GC-odorant concentration. (**A**) Single unit response to the 60 odorants, each at a different concentration. There was no correlation between unit response and GC-odorant concentration (r^2 = 0.0037; *P* = 0.65). (**B**) The effects of GC-odorant concentration on responses of all units of an ensemble (*N* = 14 units) from a single preparation. There was no significant correlation between ensemble response and odorant concentration (r^2 < 0.0001; *P* = 0.81). Response Indices were normalized for analysis.

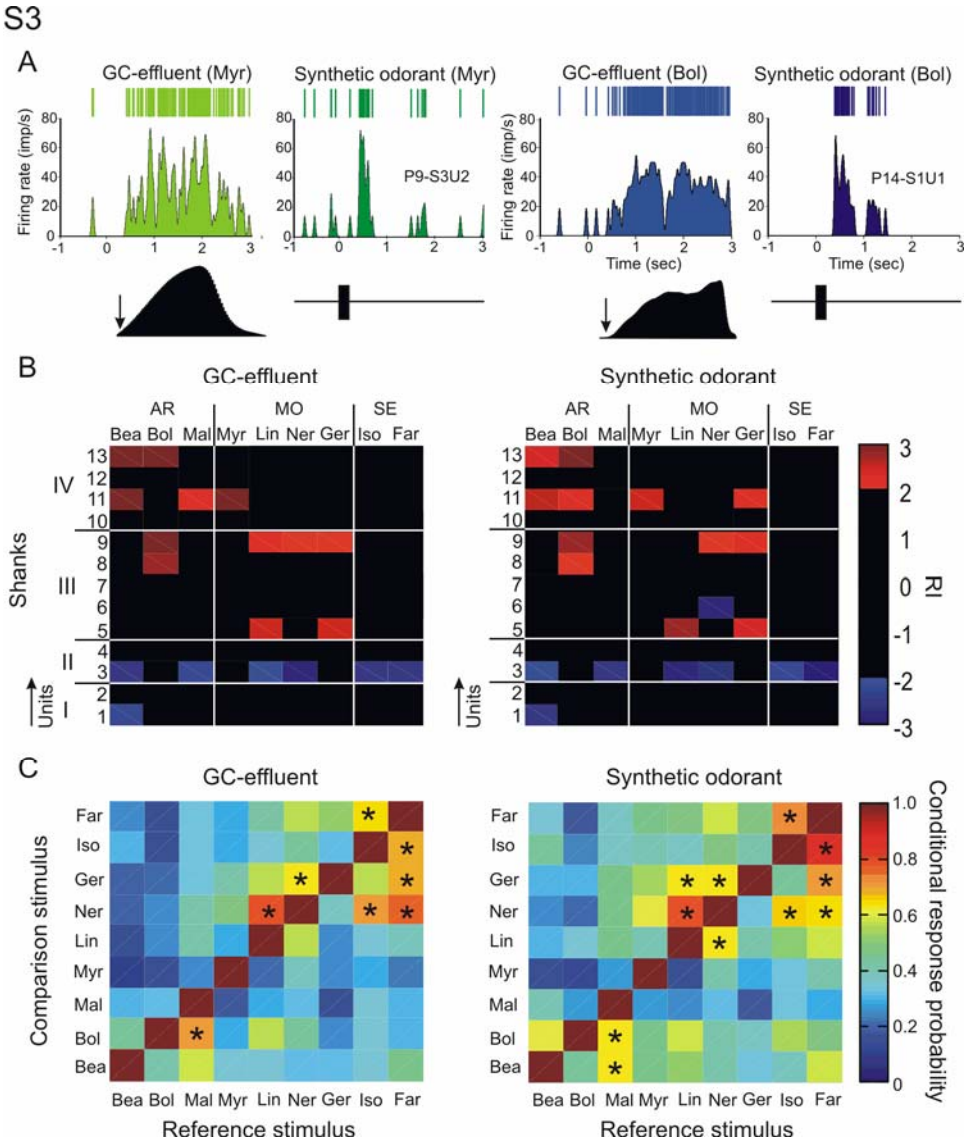

Fig. S3. Comparison between active GC-fractionated odorants from *D. wrightii* flowers and equivalent synthetic compounds. (**A**) PSTHs and raster plots of two units that show significant responses (based on CUMSUM test, see Methods) to both natural and synthetic myrcene and benzyl alcohol. Lower plots (in black) are the GC-peaks of the two compounds (left) and the synthetic stimulus pulse (right). Arrows on the GC peaks indicate stimulus onset. The 1st and 3rd columns illustrate the prolonged unit activity in response to a natural odorant pulse from the GC. A brief (200 ms) stimulus pulse of the synthetic compound, at a concentration equal to the GC eluate, leads to a brief increase in spiking rate that closely follows the stimulus duration. (**B**) Responses of one 13-unit ensemble to synthetic (*right plot*) and natural (GC eluate) (*left plot*) floral odorants, plotted as color-coded response matrices across all electrode shanks (rows I-IV) and odorants (nine columns). Tested odorants were those evoking the strongest ensemble responses: Aromatics (AR): *bea*, *bol*, *mal*; Monoterpenoids (MO): *myr*, *lin*, *ner*, *ger*; and Sesquiterpenoids (SE): *car*, and *far.* Weak or null responses were not shown, with only

the significant excitatory (RI ≥ 2.0 SD) or inhibitory (RI ≤ -2.0 SD) responses shown for clarity. (**C**) Conditional response probability for all activated units (*n* = 113) was determined separately for the synthetic and natural odorants. Asterisks denote response probabilities ≥ 0.65.

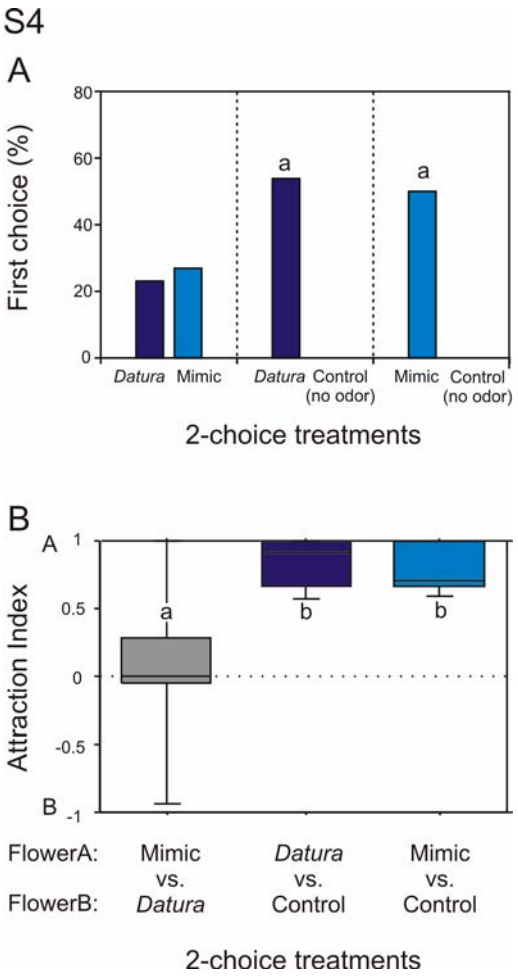

Fig. S4. Behavioral 2-choice tests examined whether the synthetic mixture of *D. wrightii* odorants identified by GCMR were as efficacious as the *D. wrightii* bouquet containing more than 60 components. (**A**) With artificial flowers, the percentages of moths that chose paper flowers emitting *D. wrightii* or the nine-component *D. wrightii* odor mimic (*left*), *D. wrightii* scent or no scent (control) (*middle*), and nine-component *D. wrightii* odor mimic or no scent (control) paper flowers (*right*). (**B**) Behavioral attraction index of the two-choice experiments. Box plots show the entire data range (error bars, 5th and 95th percentile; filled box, the 25th and 75th percentile; horizontal line, the mean). Letters denote a significant difference between odor stimuli (*G*-test: $P < 0.05$). $n = 26$ moths for each two-choice experiment.

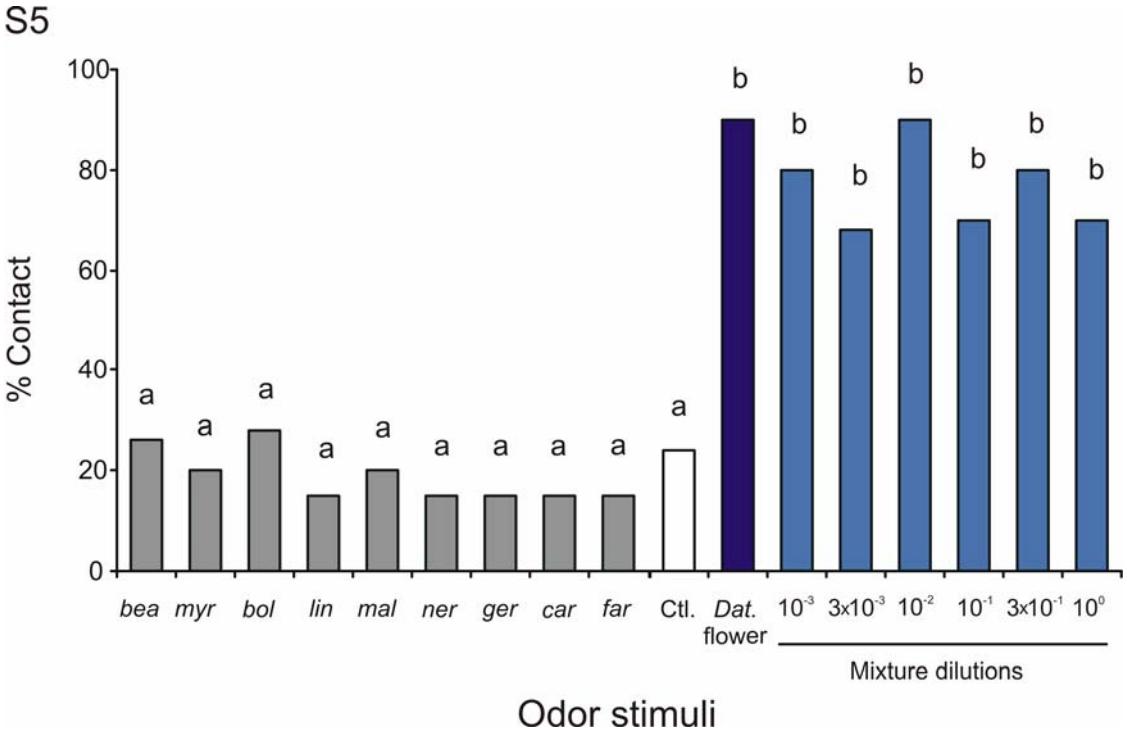

Fig. S5. The percentage of moths coming into contact with the odor source. Single odorants (grey bars) and mixtures at different concentrations (blue bars) were tested. *n* = 20–50 moths per odor stimulus treatment. Letters denote a significant difference from the (negative) mineral oil control (*G*-test: $P < 0.01$).

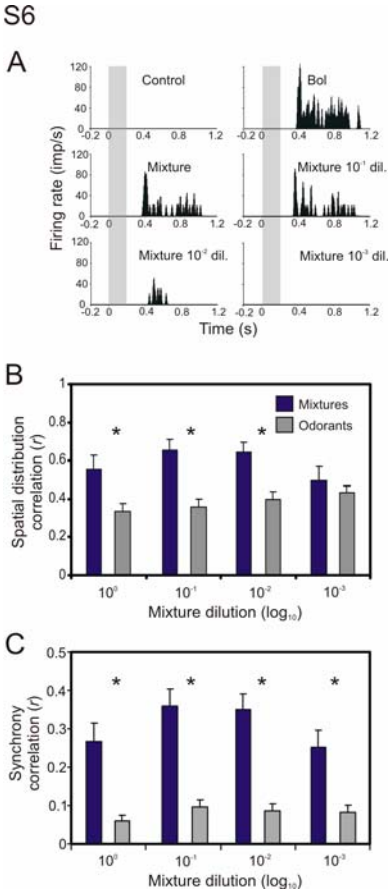

Fig. S6. Spatial processing of odor mixtures. (**A**) Unit responses to mixtures can show a dose-response relationship. In this unit, a 200-ms pulse (grey bars) of the mineral oil control does not elicit a response (*PSTH plot first row, left*) but a pulse of benzyl alcohol does (*PSTH plot first row, right*). A pulse of the odor mixture containing an equal amount of benzyl alcohol produces a near-equivalent response (*second row, left*) and with increasing mixture dilution, unit responses decrease until, at a mixture concentration of 10^{-3} , the unit no longer responds (*third row, right*). (**B**) The correlation in evoked responses from the spatial distribution of activated units between mixtures and individual odorants for all pairs of stimuli determined for all animals (n = 8, units = 113). The histograms show the mean (±SEM) correlation coefficients for the mixtures to one another (blue bars), and the correlation coefficients for the mixtures to the odorants (grey bars). (**C**) The correlations between mixture- (blue bars) and single odorant- (grey bars) evoked synchrony patterns for all animals (n = 8 moths) and units (n = 113, 750 cell pairs). Asterisks denote a significant difference (Mann-Whitney U-test: $P < 0.05$) between mixtures and single odorants.

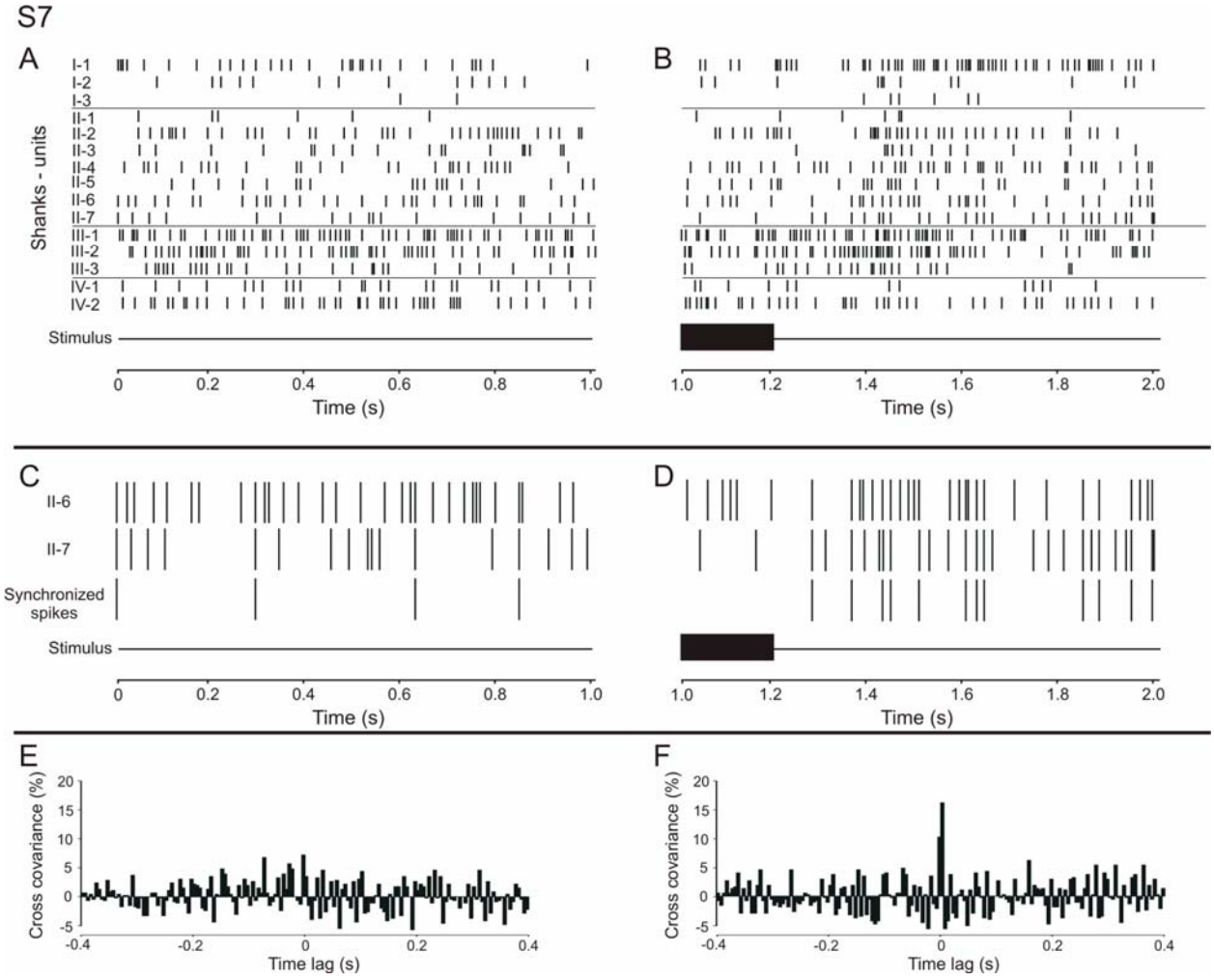

Fig. S7. Ensemble responses before and after 10^{-2} mixture stimulation. (**A**) 1 s time course of ensemble activity before odor stimulation. The ensemble response is shown as a raster plot from 15 different units. The stimulus time course is shown below raster plot. (**B**) 1 s time course during odor stimulation (200 ms). There is a 350 ms delay from the odor onset to the stimulus reaching the preparation. (**C**) The activity (as shown by the raster plot) of two units (II-6 and II-7) which show a small degree of synchronized activity (as shown by bottom rasters). (**D**) After odor stimulation, the same two units show a high degree of synchronized activity. (**E**) After shuffle subtraction (accounting for differences in firing rates between units) these two units show little cross-covariance (< 6%) before odor stimulation. (**F**) In contrast, during odor stimulation these two units are highly correlated with one another.

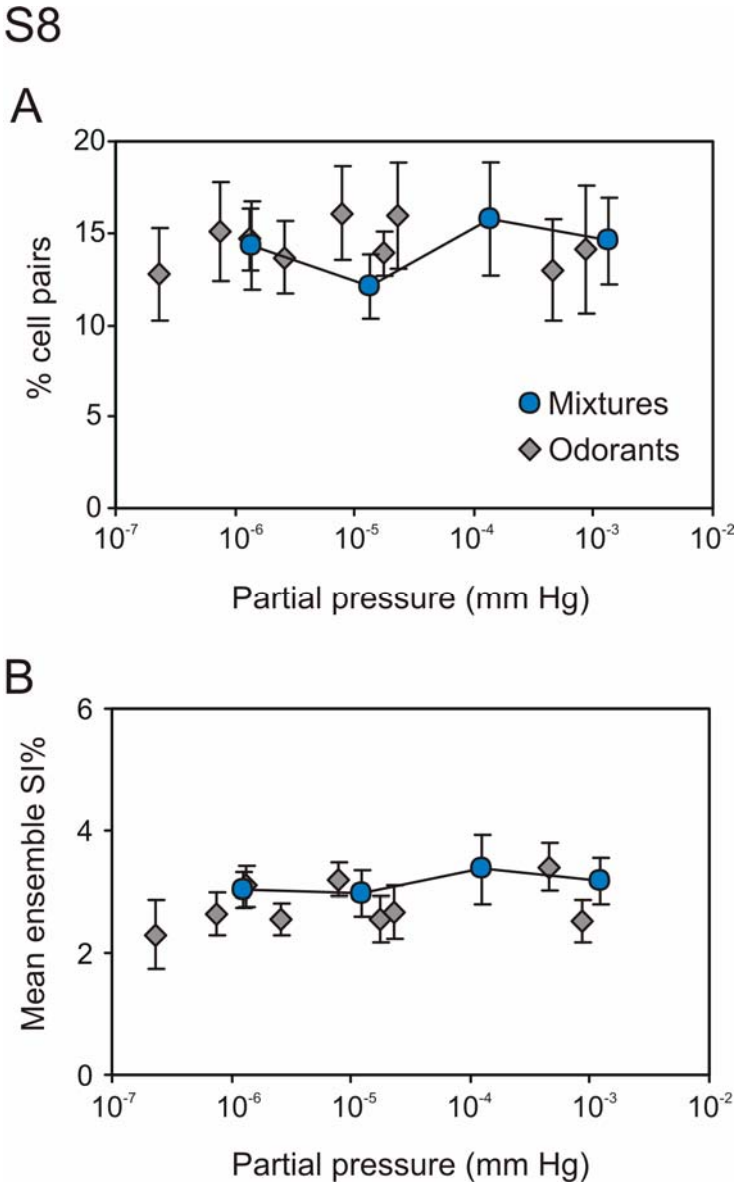

Fig. S8. Ensemble synchrony magnitude and proportion of cell pairs exhibiting synchronized spike activity as a function of stimulus intensity. (**A**) The effects of stimulus concentration on the percentage of cell pairs within each ensemble that produces a synchrony index ≥ 10% (*n* = 8 moths). (**B**) The magnitude of synchrony (SI%) produced by all cell pairs within an ensemble (*n* = 8 moths, 750 cell pairs). Blue circles correspond to the mixture stimulus (10^0 – 10^{-3} concentrations) and grey diamonds represent the individual odorants. Synchrony produced by the mixtures was not significantly different from the single odorants (multiple comparisons: $P > 0.05$). Moreover, the effects of single odorant and mixture concentrations did not affect the percentage of cell pairs contributing to the coding ensembles (mixed effects, repeated measures regression for odorants: $P = 0.27$; for mixtures: $P = 0.57$) or synchrony (for odorants: $P = 0.27$; for mixtures: $P = 0.22$).

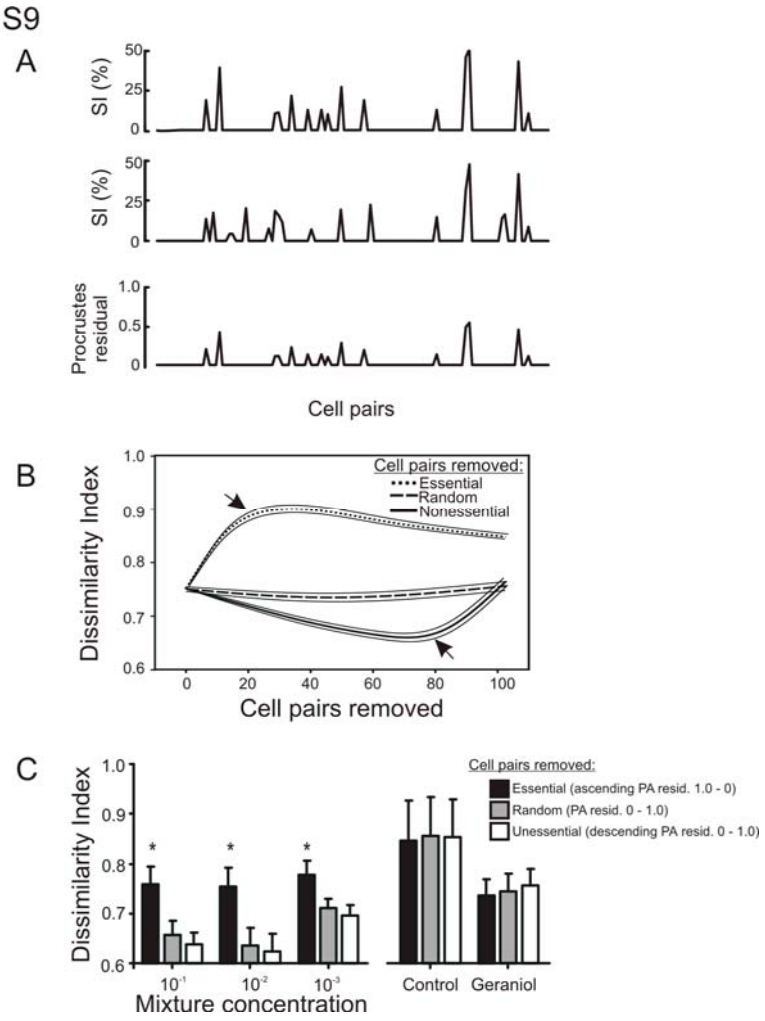

Fig. S9. Procrustes analysis of odor-evoked synchrony. (**A**) The evoked synchrony coefficients between all cell pairs (*n* = 120) in response to the 10^0 and 10^{-1} (**A**, *upper and middle traces*, *respectively*) mixtures. Note the similarity in the evoked synchrony. To quantify this similarity, we converted the synchrony coefficients for 10^0 and 10^{-1} mixture responses into two vectors and then performed a PA to compare the two vectors. The comparison provided a residual on the similarity of each cell pair, where cell pairs that are similar produce a residual approaching 1, whereas dissimilar cell pairs produce residuals approaching 0 (**A**, *lower trace*). This analysis thus provides a means to identify cell pairs which have similar synchrony responses between two stimuli. (**B**) Sensitivity analysis of the importance of specific cell pairs contributing to the mixture code. Increasing numbers of cell pairs were removed from the vectors representing the 10^0 mixture (*n* = 8 preparations) using the three different algorithms: random (solid line; using random number generator), essential (dotted line; cell pairs with ascending PA residuals 1.0 to 0), and unessential (dashed line; cell pairs with descending PA residuals 0 to 1.0). Bounded lines are ± SEM. (**C**) To determine whether a similar subset of cell pairs may encode all mixture concentrations, 20 cell pairs were removed

by the three different algorithms (black bars are essential cell pairs removed; grey bars are cell pairs removed randomly; white bars are non-essential cell pairs removed) from the synchrony coefficient vector evoked by the 10^{0} mixture stimulus. The Dissimilarity Indices between the resulting vectors and those evoked by each mixture concentration (10^{-1} – 10^{-3}) were determined. Asterisks denote a significant (Kruskal Wallis test: $P < 0.05$) difference in Dissimilarity Indices between treatments.

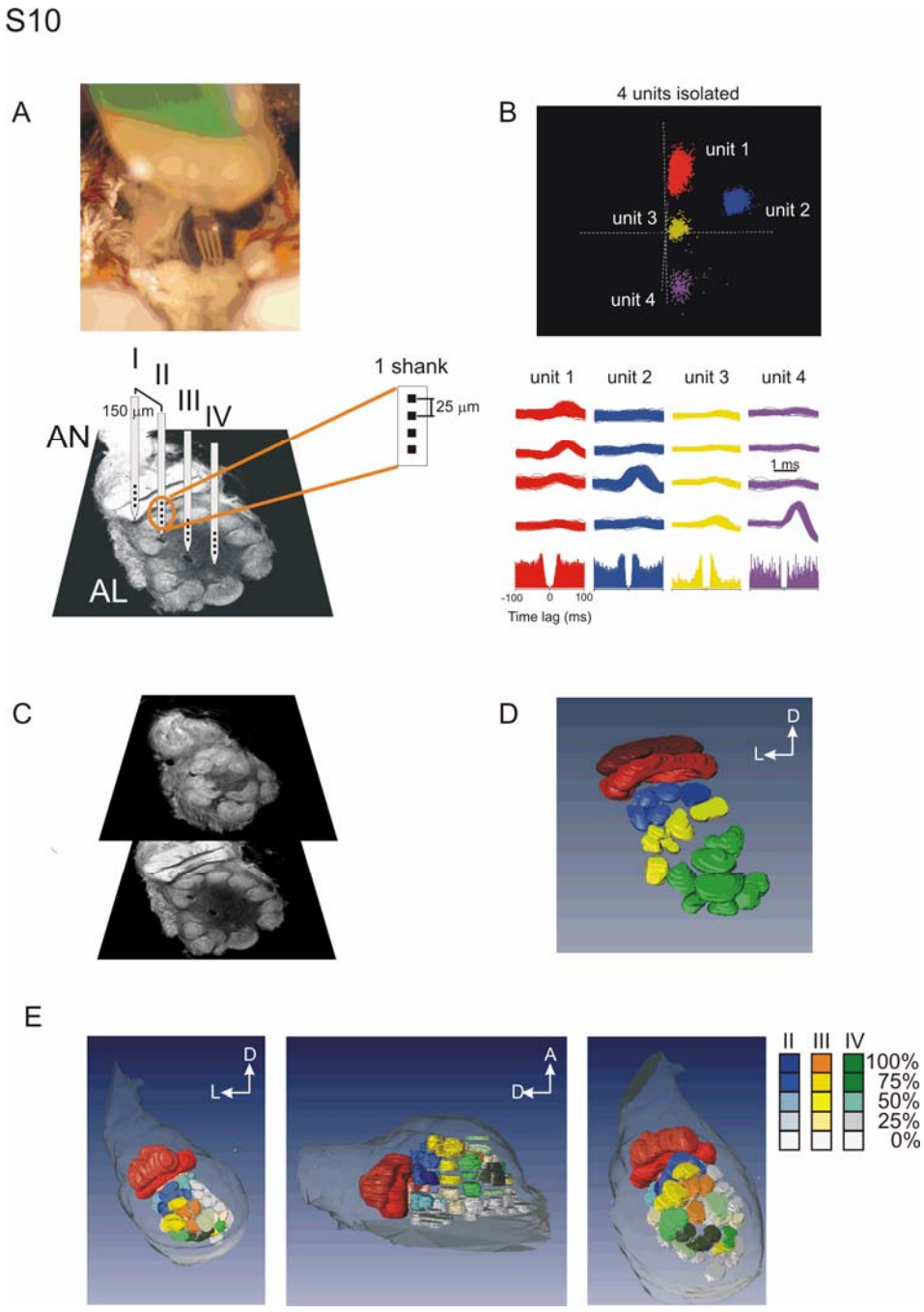

Fig. S10. Position of multiunit recording array (MR) in the moth's AL and sorting of recorded units. (**A**, *top*) The four shanks are spaced such that the array encompasses a large volume of the AL. (**A**, *bottom*) Positioning of the four channels on each shank provided recording of broad zones within processing glomeruli and neuropil. (**B**, *top*) Neural activity was recorded on each of the four channels, plotted in 3-dimensional space, and sorted according to waveform characteristics. (**B**, *bottom*) Isolated neural

units recorded from each of the four channels. Autocorrelograms demonstrate the refractory period for each neural unit. Time bin = 1 ms. (**C**) 2 images from the confocal image stack demonstrating the top and middle portions of the AL. Glutaraldehyde staining of the AL and confocal microscopy provided determination of the positions of each of the MR shanks and the depth in which the MR was inserted into the AL. (**D**) From confocal image stacks, the glomeruli that the MR shanks impaled or were adjacent to could be determined for each preparation. Blue glomeruli correspond to shank II, yellow for shank III, and green for shank IV. Shank I was placed in the MGC-T1 (MGC shown in red). (**E**) The cumulative placement of the MR probe for all 8 preparations. The position of the probe was consistent between preparations as demonstrated by the impaled glomeruli occupying the lateral region of the AL (right and leftmost panels) and the depth in which the probe was placed in the AL (middle panel). The MR shanks were consistently placed in the lateral side of the AL, and at a posterior-to-anterior depth of ca. 200 μm. The color scale denotes the frequency that glomeruli were impaled or adjacent to the shanks for all preparations, e.g., deep blue glomeruli correspond to those glomeruli being impaled by shank II 100% of the time (8/8 of the preparations). Glomeruli not localized near the shanks are shown in white.